APPLICATION OF SUSPENSION SYSTEM FOR ROBOTIC GRINDING BY LOW POWER ROBOT

Mohammad Jashim Uddin*
Science of Production and Environment, Graduate School of Science and Engineering,
Saitama University, 255 Shimo-Okubo, Saitama 338-8570, Japan
Yasuo Nasu
Department of Mechanical Systems Engineering, Graduate School of Science and Engineering,
Yamagata University, Jonan 4-3-16, Yonezawa 992-8510, Japan

Abstract During the grinding operation by a robot in the vertical plane, a large actuator torque is required due to the enormous gravity force effect of the tools and the robot arm. A new grinding strategy has been developed for a low power robot in the vertical plane using a suspension system, where the lifting force of spring balancer compensates the gravity force of the tools and the robot arm. For robotic grinding, to achieve position and force tracking simultaneously, this paper shows the hybrid position/force control strategy with respect to the dynamic behavior of the spring balancer. To show the effectiveness of the proposed system, simulation and experiment have been carried out by a 2 DOF manipulator with a suspension system.

Keywords: Direct drive motor, Suspension system, Spring balancer, Hybrid control, Robotic grinding.

INTRODUCTION

In industry, suspension systems are used for heavy object manipulation in various ways. Recently, using air balancer, up to 300kg mass can be manipulated safely. In Australia, for sheep shearing process, human uses suspension system to relieve from enormous physical work. The essence of heavy object manipulation by using the limited physical power of human body is the suspension system. For heavy object manipulation by a low power robot there are some problems, like, the limitation of actuators torque and the limitation of the force sensor. We have proposed that like human being by using suspension systems a low power robot is also able to perform heavy tasks with small capacity force sensor and low power actuators. Fig. 1 shows some examples of suspension systems used by human.

Industrial robots play an important role for grinding operation in the automation process. Most of the grinding robots operate in a constrained environment. Force controlled grinding robots were developed by many researchers (Whitney, 1977, Whitney and Brown, 1987, and Kashiwagi *et. al.*, 1990,). Automated robotic deburring has been described in (Kazerooni *et. al.*, 1986 and Her and Kazerooni, 1991). In all the previous deburring or grinding researches, the weight of grinding tools and the gravity effect of the robot arm were not the compensation for gravity was not considered. In the vertical plane, the grinding operation is very difficult due to the gravity effect of the robot arm, especially when the actuator torque limit is beyond the range of gravity effect. Nasu *et. al.*, 1999, proposed the considered. There are some researches on robot arm manipulation in the vertical plane (Nemec, 1994), but Suspended Robot Grinding System (SRGS) In order to ensure heavy grinding tasks and precise grinding surface quality by a low powered manipulator. Uddin *et. al.*, 2000, proposed Suspended Tool System (STS) and Suspended Robot Arm System (SRAS) for heavy tools manipulation in the horizontal plane and for heavy robot arm manipulation in the vertical plane, respectively. Suspension system has many advantages compared to the conventional system. It can manipulate the robot arm beyond the range of actuator's torque limit by utilizing the lifting force of the spring balancer. The joint friction is less than the conventional system. It creates a smaller force effect on the wrist joint, which is in favor of the small capacity force sensor.

In robotic grinding, robots are usually operated in a constrained environment. So, it is necessary to control the position of end-effector in the free direction and the contact force in the constrained direction. The hybrid position/force control scheme proposed by Raibert and Craig, 1981, has gained considerable popularity over the other control schemes. In this paper, hybrid position/force control strategy of the manipulator is described with the dynamic effects of the spring balancer for robotic grinding.

*Email: jashim@mech.saitama-u.ac.jp

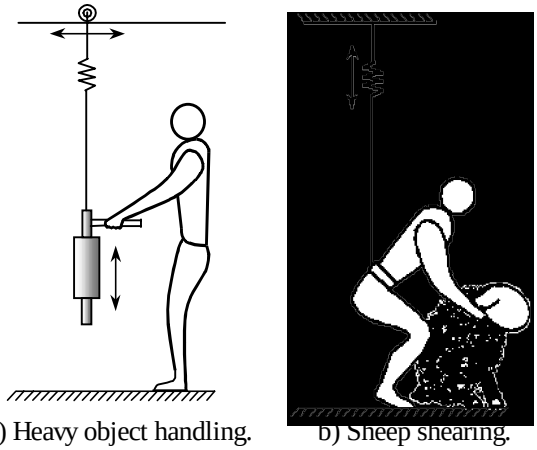

a) Heavy object handling. b) Sheep shearing.

Fig.1 Examples of suspension system used by human

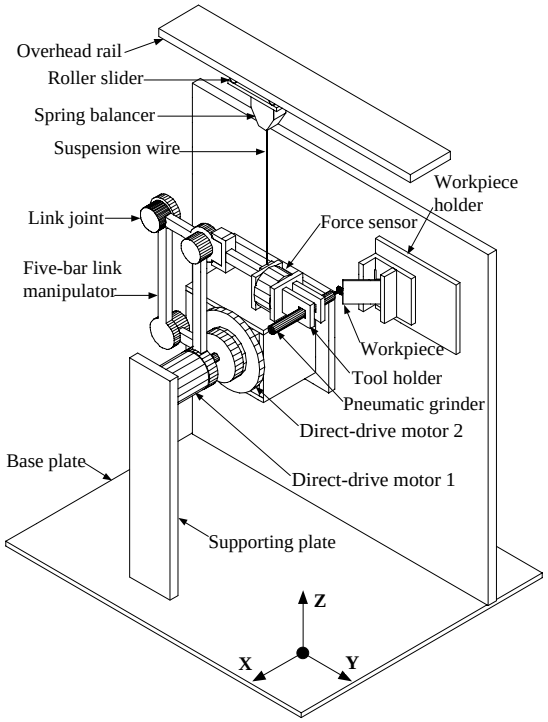

Fig. 2 A low power robot with suspension system

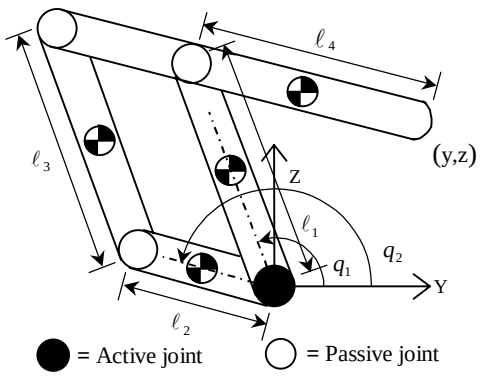

Fig. 3 Closed-loop five-bar link mechanism

Table –1 Link Properties

Properties	Link1	Link2	Link3	Link4
Length [m]	0.26	0.12	0.26	0.12+0.26
Mass [kg]	0.43	0.60	0.72	1.413
C.M [m]	0.154	0.038	0.130	0.074
M.I [kg.m^2]	0.005	0.002	0.010	0.0231

ROBOT SYSTEM

The robot arm can be driven directly or indirectly. With direct drive, the link joint is coupled to the rotor of the driving motor directly. With indirect drive, the link is connected to the driving motor through a transmission mechanism. Direct drive method provides better positioning accuracy since the intermediate gearing system is eliminated and consequently the mechanism is free of backlash and hysteresis. Another advantage is the improved reliability because of the smaller number of mechanical parts. Direct drive arms, in general, tend to have excessively fast operating ranges, whereas the output forces are extremely small (Asada and Ro, 1985). The experimental system consists of a robot with two degrees of freedom (DOF) having a five-bar link configuration and a suspension mechanism. The robot arm can move in the vertical plane (Y-Z plane). The suspension system consists of a spring balancer and an overhead rail. A roller slider moves on the overhead rail freely with the spring balancer. The overhead rail acts as a positioning device. The spring balancer suspends the manipulator and the tools by its lifting force. The lifting force of the spring can adjust easily by an adjusting screw manually. Here it is important to note that the lifting force of the spring balancer must be equal to the gravity forces of the manipulator and the tools, otherwise it will affect the motion of the manipulator severely. Fig. 2 shows the CAD design of direct drive five-bar parallel manipulator with a suspension system. Table 1 shows some important properties of five-bar link mechanism.

Five-bar Link Mechanism

In parallelogram configuration, the five-bar linkage is one of the most common in use. The five-bar manipulator consists of four linkages to form a closed-loop kinematics chain structure. In the theory of mechanisms it is a convention to count the ground as an additional linkage, which explains the terminology. In the five-bar manipulator, two direct drive motors directly coupled with two input links. There is no transmission mechanism (e.g., gear, belt etc.) between input link and driving motor. The five-bar manipulator is a revolute type because, the driving motors produce a pure rotary motion of the manipulator through the input links. A closed-loop five-bar link mechanism is shown in Fig. 3. There are two input links that are driven by two independent direct drive motors. Both the motors are fixed to a base frame. The length of links 1, 2, 3, and

4 are denoted by ℓ_1, ℓ_2, ℓ_3, and ℓ_4, respectively. The angles of the input links are denoted by q_1 and q_2 measured from Y-axis. The end point coordinates are:

$$y = \ell_1 \cos q_1 - \ell_4 \cos q_2 \quad (1)$$

$$z = \ell_1 \sin q_1 - \ell_4 \sin q_2 \quad (2)$$

To avoid redundancy, the inverse kinematics of the manipulator is obtained from equation (1) and (2) as:

$$q_1 = a\tan 2\left(\frac{z}{y}\right) + a\cos\left[\frac{\ell_4^2 - y^2 - z^2 - \ell_1^2}{2\ell_1\sqrt{y^2+z^2}}\right] \quad (3)$$

$$q_2 = a\tan 2\left(\frac{z}{y}\right) + a\cos\left[\frac{\ell_4^2 + y^2 + z^2 - \ell_1^2}{2\ell_4\sqrt{y^2+z^2}}\right] \quad (4)$$

The task space Jacobian matrix is a 2×2 matrix, which is obtained from equation (1) and (2) as:

$$\mathbf{J}(\mathbf{q}) = \begin{bmatrix} -\ell_1 \sin q_1 & \ell_4 \sin q_2 \\ \ell_1 \cos q_1 & -\ell_4 \cos q_2 \end{bmatrix} \quad (5)$$

The inertia matrix of the manipulator is a 2×2 matrix and can be expressed as:

$$\mathbf{M}(\mathbf{q}) = \begin{bmatrix} I_1 + m_1\ell_{C1}^2 + I_3 + m_3\ell_{C3}^2 + m_4\ell_1^2 & (m_3\ell_2\ell_{C3} - m_4\ell_1\ell_{C4})\cos(q_2 - q_1) \\ (m_3\ell_2\ell_{C3} - m_4\ell_1\ell_{C4})\cos(q_2 - q_1) & I_2 + m_2\ell_{C2}^2 + I_4 + m_4\ell_{C4}^2 + m_3\ell_2^2 \end{bmatrix} \quad (6)$$

where I_k, m_k, ℓ_k, and ℓ_{Ck} (k=1,…,4)are the inertia, mass, length, and center of mass of the links, respectively.

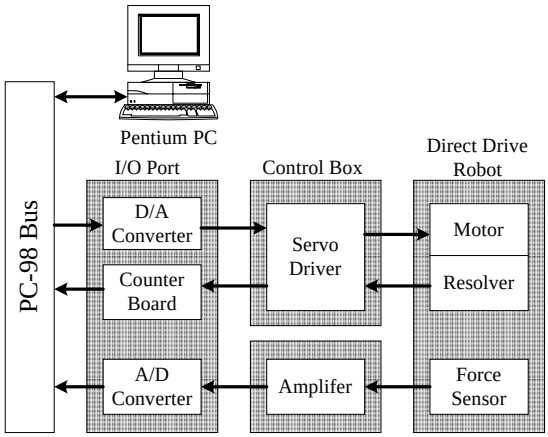

Fig. 4Hardware of robot system

Table –2 Properties of direct drive motors

Properties	Motor 1	Motor 2
Torque [Nm]	**2.0**	**3.9**
Rated RPS	4.5	4.5
Encoder [p/rev]	102400	102400
Weight [kg]	2.4	4.5
Inertia [kg.m^2]	2.0 x 10^{-3}	2.0 x 10^{-3}

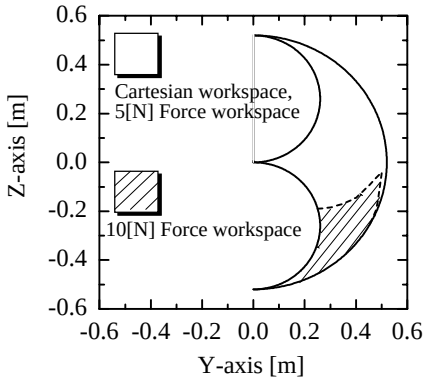

Fig.5 Cartesian and force workspace

The Coriolis and centripetal force matrix is a 2×1 matrix and can be expressed as:

$$\mathbf{H}(\mathbf{q}, \dot{\mathbf{q}}) = \begin{bmatrix} (m_4\ell_1\ell_{C4} - m_3\ell_2\ell_{C3})\sin(q_2 - q_1)\dot{q}_2^2 \\ (m_3\ell_2\ell_{C3} - m_4\ell_1\ell_{C4})\sin(q_2 - q_1)\dot{q}_1^2 \end{bmatrix} \quad (7)$$

The gravity matrix is a 2×1 matrix and expressed as:

$$\mathbf{G}(\mathbf{q}) = \begin{bmatrix} (m_1\ell_{C1} + m_3\ell_{C3} + m_4\ell_1)g\cos q_1 \\ (m_2\ell_{C2} + m_3\ell_2 - m_4\ell_{C4})g\cos q_2 \end{bmatrix} \quad (8)$$

where g is the acceleration due to the gravity.

Hardware Description

A hardware schematic diagram of the control system is shown in Fig. 4. It illustrates the various connections between the controller and the components of the system. A Pentium based microcomputer (NEC, PC-98), 133 MHz, is used in the control system. The A/D and D/A converter has 8 channels and 12-bit resolution. The feature of servo driver is that it can be preset to operate in three different modes of control, i.e. position control, velocity control, and torque control. For our experimental system, the servo driver is set to the torque control mode. The counter board has 3 ports and 24-bit pulse resolution. A low capacity three-axis force sensor is mounted between the end of robot arm and the tool holder, which is calibrated to work up to 19.62N. An operational amplifier with low pass filter is designed to eliminate unexpected noise from the output signal of the force sensor. Table 2 shows some important properties of direct drive motors.

Work Space and Singularity Problem

Asada and Ro (1985) and Ting (1992) pointed out the singularity problem for the five-bar closed link manipulator. The Cartesian workspace of a robot arm is the total volume swept out by the end-effector as the robot arm executes all possible motions. The Cartesian workspace is constrained by the geometry of robot arm. The force workspace of a robot arm is the total volume swept out by the end-effector as the robot arm executes all possible motions with a specific force at the end-effector, the normal force and the tangential force. The force workspace is constrained by the normal and tangential force applied at the end-effector. Actually, the force workspace is a sub set of the Cartesian workspace.

For a given end-effector position, there are in general two possible solutions to the inverse kinematics. The singular configuration separates these two solutions. At singular configuration, the manipulator can not move in certain directions. There are two types of singularities, stationary singularity and uncertainty singularity. A closed-loop manipulator may have both stationary and uncertainty singularities. At a stationary singularity, the Jacobian matrix has zero determinant, whereas at an uncertainty singularity, the determinant of Jacobian matrix is infinity. For the five-bar link configuration, the determinant of Jacobian matrix $\mathbf{J}$, is defined as:

$$|\mathbf{J}| = \ell_1 \ell_4 \sin(q_2 - q_1) \tag{9}$$

The stationary singularity occurs when:

$$\sin(q_2 - q_1) = 0 \tag{10}$$

From equation (10), the stationary singularity occurs on the boundary of the workspace. Thus, by selecting link dimensions, a wide singularity free workspace can be obtained. Fig. 5 shows the simulated Cartesian workspace and force workspace of the five-bar link mechanism in the vertical plane when the lifting force of the spring balancer is setup to a force of 9.81N and the actuator rotations were constrained within the range: $0^o \le q_1 \le 180^o$ and $180^o \le q_2 \le 360^o$. The total Cartesian workspace copes with 5.0N force workspace, where the 10.0N force workspace is a subset of the Cartesian workspace.

ROBOT CONTROL DYNAMICS

If the end-effector of the manipulator is in contact with the environment, the dynamic equation of the manipulator in the Cartesian spaces can be written as:

$$\begin{aligned} \boldsymbol{f} = {} & \mathbf{M}(\mathbf{q})\mathbf{J}^{-1}(\mathbf{q})[\ddot{\mathbf{x}}^d + k_v(\dot{\mathbf{x}}^d - \dot{\mathbf{x}}) + k_p(\mathbf{x}^d - \mathbf{x})] - \\ & \mathbf{M}(\mathbf{q})\mathbf{J}^{-1}(\mathbf{q})\dot{\mathbf{J}}(\mathbf{q})\dot{\mathbf{q}} + + \mathbf{H}(\mathbf{q},\dot{\mathbf{q}}) + \mathbf{G}(\mathbf{q}) + \mathbf{F}(\mathbf{q})_f + \\ & \mathbf{J}^T(\mathbf{q})\boldsymbol{f}^d + \mathbf{J}^T(\mathbf{q})k_f \int_0^t (\boldsymbol{f}^d - \boldsymbol{f}) dt \end{aligned} \tag{11}$$

where $\mathbf{M}(\mathbf{q}) \in R^{2\times 2}$ denotes the symmetric and positive definite inertia matrix of the links; $\mathbf{H}(\mathbf{q},\dot{\mathbf{q}}) \in R^{2\times 1}$ denotes the vector of nonlinearities which includes the Coriolis and centripetal forces; $\mathbf{G}(\mathbf{q}) \in R^{2\times 1}$ denotes the gravity force; $\mathbf{F}(\mathbf{q})_f \in R^{2\times 1}$ denotes the joint friction; $\mathbf{J}(\mathbf{q}) \in R^{2\times 2}$ is the task space Jacobian matrix; $\ddot{\mathbf{x}} \in R^{2\times 2}$ and $\boldsymbol{f}^d \in R^{2\times 2}$ are the vectors of auxiliary position and force inputs, respectively. $\mathbf{x}^d \in R^{2\times 2}$ and $\boldsymbol{f}^d \in R^{2\times 2}$ are the reference position and force vector, respectively. k_p, k_v, and k_f are the position, velocity, and force gain factor, respectively.

In the robot arm suspension system, spring balancer acts as a gravity force compensator. A balanced suspension environment is required for the safe robot arm manipulation. At a balanced suspension, the gravity force and the friction force of the manipulator must be equal to the lifting force of the spring balancer. The required condition is as follows:

$$\mathbf{G}(\mathbf{q}) + \mathbf{F}(\mathbf{q})_f = \mathbf{J}^T(\mathbf{q})\mathbf{F}_b \tag{12}$$

where $\mathbf{F}_b \in R^{2\times 1}$ denotes the lifting force.

Based on the equation (11) and (12), linearized and decouple feedback control equation is as follows:

$$\begin{aligned} \boldsymbol{f} = {} & \mathbf{M}(\mathbf{q})\mathbf{J}^{-1}(\mathbf{q})[\ddot{\mathbf{x}}^d + k_v(\dot{\mathbf{x}}^d - \dot{\mathbf{x}}) + k_p(\mathbf{x}^d - \mathbf{x})] - \\ & \mathbf{M}(\mathbf{q})\mathbf{J}^{-1}(\mathbf{q})\dot{\mathbf{J}}(\mathbf{q})\dot{\mathbf{q}} + \mathbf{H}(\mathbf{q},\dot{\mathbf{q}}) + \mathbf{G}(\mathbf{q}) + \mathbf{F}(\mathbf{q})_f - \\ & \mathbf{J}^T(\mathbf{q})\mathbf{F}_b + \mathbf{J}^T(\mathbf{q})\boldsymbol{f}^d + \mathbf{J}^T(\mathbf{q})k_f \int_0^t (\boldsymbol{f}^d - \boldsymbol{f}) dt \end{aligned} \tag{13}$$

Fig. 6 shows the block diagram of hybrid control system.

SIMULATION RESULTS

A low powered manipulator cannot move in the vertical plane, especially when the actuators torque limit is not sufficient to overcome the gravity force of the manipulator and the tools. For this reason, the lifting force is essential to compensate the gravity force. To manipulate the robot arm in the vertical plane within the maximum torque limit, the characteristic graph is necessary to know the required lifting force. Fig. 7 shows the characteristic graph, which expresses the relationship between the lifting force of spring balancer and the actuator's torque at the velocity of 0.01m/sec. In this graph, the actuator torque is increased by the influence of the lifting force. The characteristic graph shows that the robot arm can be manipulated safely within the torque limits when the lifting force of the spring balancer varies from 5.2 N to 12.0 N.

Hybrid position/force control simulations have been carried out for robotic grinding system. In this simulation, total manipulation time is t_f=10.0sec, where the blend time is t_b=0.5sec. The commanded velocity is v=0.01m/sec. From the characteristic graph (Fig. 7), the lifting force is considered as F_b=12.0N. The desired force is $\boldsymbol{f}^d$=5.0N. In the vertically upward motion, the manipulator tracks on a constrained surface from (0.3, 0.0) to (0.3, 0.1). Fig. 8 shows that the lifting force of the spring balancer and the gravity force of the manipulator when the manipulator moves vertically upward. This simulation result shows that in the vertical motion, the lifting force compensates a big portion of gravity force of the manipulator and consequently the effective force is very small.

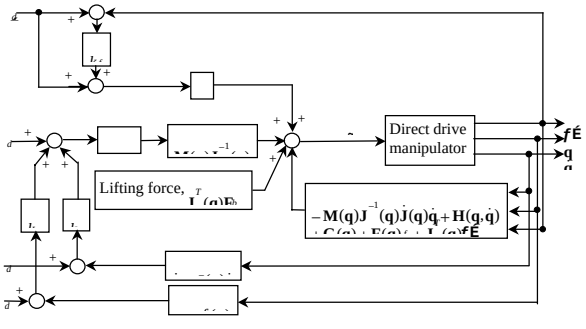

Fig.6 Hybrid position/force control model

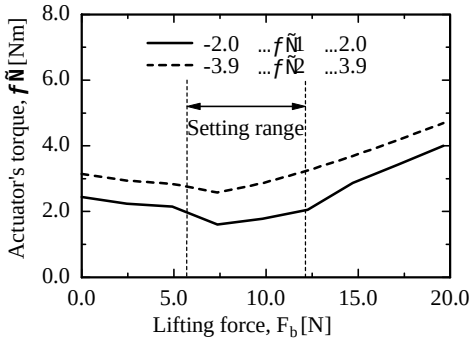

Fig. 7 Characteristic graph

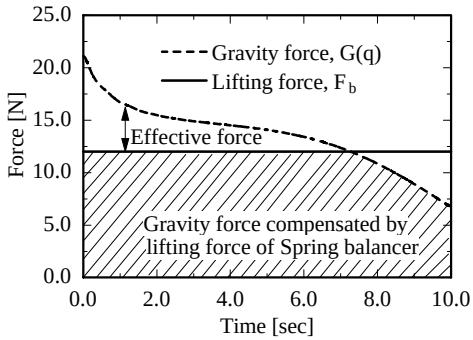

Fig. 8 Compensation of gravity force by the lifting force

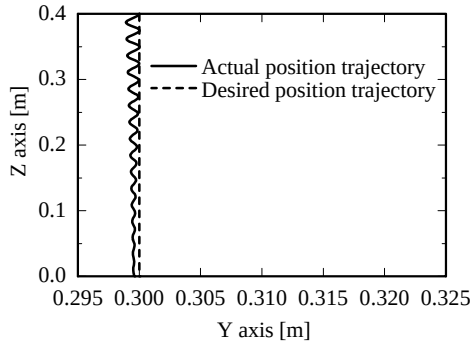

Fig. 9 Hybrid position trajectory

Fig. 9 and Fig. 10 show the simulation result of hybrid position trajectory and hybrid force trajectory, respectively. Simulation results show that the position output tracks the desired position trajectory with a small steady state error and the force output goes to the desired force trajectory after a short time. Fig. 11 shows actuator's torque trajectory when the manipulator moves in the vertical plane. This result shows that both actuator's torque are within the maximum torque limit.

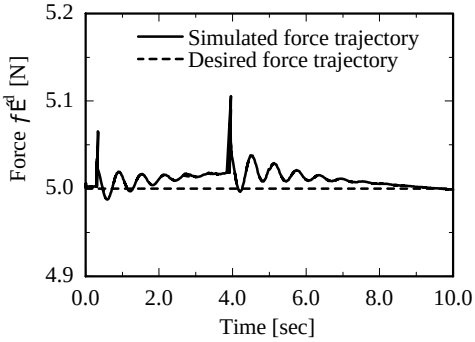

Fig. 10 Hybrid force trajectory

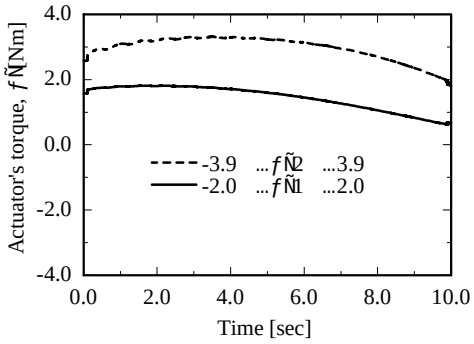

Fig. 11 Simulated actuator's torque trajectory

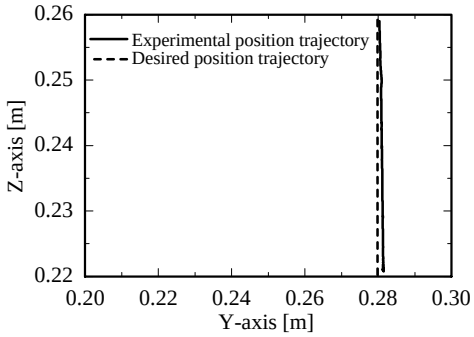

Fig. 12 Hybrid controlled position trajectory

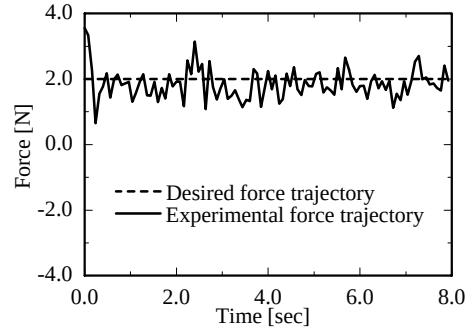

Fig. 13 Hybrid controlled force trajectory

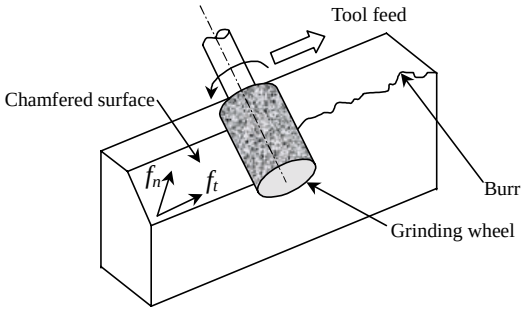

Fig. 14 Schematic diagram of chamfering operation

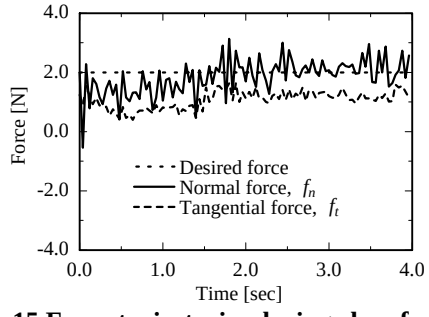

Fig. 15 Force trajectories during chamfering operation

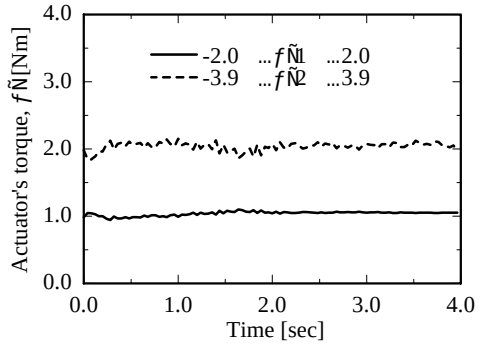

Fig. 16 Torque trajectories during chamfering operation

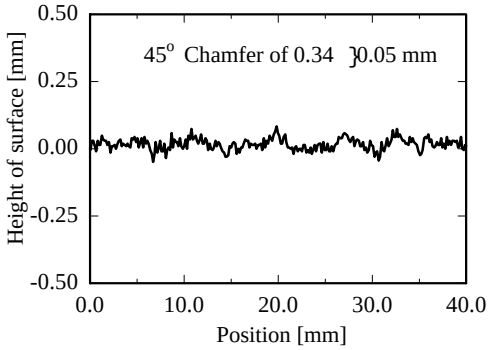

Fig. 17 Profile of chamfered surface

EXPERIMENTAL RESULTS

In the hybrid position/force control experiment, the manipulator tracks on a constrained surface from (0.28, 0.22) to (0.28, 0.26) by grasping a pneumatic grinder of weight m_t=0.35kg. To suspend the robot arm the lifting force of spring balancer is setup to F_b=12.0N, according the characteristic graph (Fig. 7). Before the experiment starts, the pneumatic grinder is in contact with a constraint surface at static condition. The commanded velocity is v=0.005m/sec. The desired force is ƒÉ=2.0N. Fig. 12 and Fig. 13 show the hybrid controlled position trajectory and hybrid controlled force trajectory, respectively. Experimental results show that in the vertical plane a low powered manipulator can manipulate safely and precisely by utilizing the lifting force of the spring balancer. Fig. 12 shows that the actual position trajectory tracks the desired position trajectory with a small steady state error. Fig. 13 shows that the actual force goes to the desired force trajectory after a very short time.

To allow the proper fitting of assembled parts and to ensure safe and proper functioning of machined parts chamfering operation is essential. Fig. 14 shows a schematic diagram of the chamfering operation. In our experimental system, the spring balancer is setup to a lifting force of F_b=12.0N to suspends the low powered robot arm. A pneumatic grinder of m_t=0.13kg with mounted point grinding wheel (WA80, 16mm diameter) has been employed in the down-cut grinding operation at the maximum rotational speed of 30000rpm. Fig. 15 shows the normal grinding force trajectory, f_n, and tangential grinding force trajectory, f_t, at a commanded velocity v=0.01m/sec during the chamfering operation on the material SS400. The experimental result shows that the normal grinding force, f_n, remains at the desired force level of ƒÉ=2.0 N because there is no significant variation in burr size. The tangential force, f_t, is about half of the normal force. Fig. 16 shows the actuator's torque trajectories during the chamfering operation on the material SS400. This experimental result shows that both actuator's torque are within the safe torque limit. Fig. 17 shows the profile of the chamfered surface of the material SS400. The chamfering result shows a chamfer width of 0.36±0.05mm. This chamfering result is within an acceptable geometric tolerance.

The experimental results of hybrid position/force control system show that a low powered robot arm can manipulate safely using the lifting force of spring balancer in the vertical plane. The experimental results of robotic grinding by a low powered manipulator shows precise surface quality, which proof that heavy grinding tasks is possible by a low powered manipulator in the vertical plane for industrial applications.

CONCLUSION

When a manipulator moves in the vertical plane, it requires a very big actuator torque due to the enormous gravity force effect of the tools and the robot arm. For this reason, robotic grinding by a robot system in the vertical plane is really very difficult. We have proposed a simple and available system for robotic grinding by a low power robot with a suspension system. For robotic grinding, to achieve position and force tracking simultaneously, we have developed the hybrid position /force control strategy with respect to the dynamic behavior of the spring balancer.

By using the presented dynamic formulation, simulations and experiments have been carried out to show the effectiveness of the proposed system. To manipulate the robot arm in the vertical plane within the maximum torque limit the characteristic graph has been developed to know the required lifting force of the spring balancer. The simulation results also show that by suspension system the manipulator can move with a small position and force error and both actuators are within the torque limit. The grinding operation has been carried out on the material SS400. The experimental results of hybrid position/force control show that the low powered robot can manipulate safely using the lifting force of spring balancer. The experimental results of chamfering operation show that heavy grinding tasks are possible by a low powered manipulator in the vertical plane. The result of the chamfered surface proves that the proposed system can guarantee a high quality surface for industrial applications.

ACKNOWLEDGEMENT

Authors are gratefully acknowledged to Dr. Toshio Kasai, Professor, Dr. Junichi Ikeno, Associate Professor, Graduate School of Science and Engineering, Saitama University, Japan for their valuable comments and critical analysis of this research work.

REFERENCES

Asada, H. and Ro, I.H., "A link design for direct-drive robot arms", *ASME Journal of Mechanisms, Transmission, and Automation in Design*, Vol. 107, No. 4, pp. 536-40, (1985).

Her, M.G. and Kazerooni, H., "Automated robotic deburring of parts using compliance control", *Transaction on ASME Journal of Dynamics Systems, Measurement, and Control*, Vol. 113 No. 1, pp. 60-6, (1991).

Kashiwagi, K., Ono, K., Izumi, E., Kurenuma, T. and Yamada, K., "Force control robot for grinding", *Proceeding of IROS'90*, pp. 1001-6, (1990).

Kazerooni, H., Bausch, J. J., and Kramer, B. M., "An approach to automated deburring by robot manipulators", *Transaction on ASME Journal of Dynamic Systems Measurement and Control*, Vol. 108, No. 4, pp. 354-359, (1986).

Nasu, Y., Uddin, M.J., Hariu, Y, Satou, H., and Mitobe, K., "Robotic grinding using suspension system", *Proceeding of the 3rd International Conference on Abrasive Technology (ABTEC99)*, pp. 88-95, (1999).

Nemec, B., "Control of redundant manipulator with limited torque", *Proceeding of IFAC Robot Control*, pp. 401-6, (1994).

Raibert, M.H. and Craig, J.J., "Hybrid position/force control of manipulators", *Transaction on ASME Journal of Dynamics Systems, Measurement, and Control*, Vol. 102 No. 6, pp. 126-33, (1981).

Ting, K.L., "Gross motion and classification of manipulators with closed-loop, four-bar chains", *The International Journal of Robotics Research*, Vol. 11 No. 3, pp. 238-47, (1992).

Uddin, M.J., Nasu, Y., Mitobe, K., and Yamada, K., "Application of suspension mechanism for low-powered robot tasks", *The International Journal of Industrial Robot*, Vol. 27, No. 3, pp. 206-16, (2000).

Whitney, D.E., "Force feedback control of manipulator fine motions", *Transaction on ASME Journal of Dynamic Systems, Measurement, and Control, Vol. 99*, No. 2, pp. 91-97, (1977).

Whitney, D.E. and Brown, M.L., "Metal removal models and process planning for robot grinding", *Proceeding of 17th ISIR*, pp. 19-29, (1987).